

Non-sacrificial template synthesis of Cr_2O_3 -C hierarchical core/shell nanospheres and their application as anode materials in lithium-ion batteries†

Ling-Yan Jiang,^{ab} Sen Xin,^{ab} Xing-Long Wu,^{ab} Hong Li,^c Yu-Guo Guo^{*ab} and Li-Jun Wan^{ab}

Received 13th April 2010, Accepted 10th June 2010

DOI: 10.1039/c0jm01027h

Cr_2O_3 -based nanospheres have been synthesized by a facile soft-template assisted method without sacrificing the template. Two types of Cr_2O_3 materials, the Cr_2O_3 -C composite nanospheres (referred to as Cr_2O_3 -C) with a novel hierarchical core/shell structure, and pure mesoporous Cr_2O_3 spheres (referred to as mesoporous Cr_2O_3) have been obtained by using a certain thermal treatment without adding more carbon precursor. The carbon coating layers in the Cr_2O_3 -C composite distribute from the inside to the surface of the spheres continuously. Both the Cr_2O_3 -C composite and the pure mesoporous Cr_2O_3 spheres are investigated with XRD, SEM, TEM, and electrochemical tests toward lithium storage. It is found that the reversible capacity for Cr_2O_3 -C composite still retain more than 600 mA h g⁻¹ even after 35 cycles, showing a capacity retention of 87%, while mesoporous Cr_2O_3 spheres and commercial Cr_2O_3 can only deliver a capacity of 320 mA h g⁻¹ and 280 mA h g⁻¹, respectively. The improvements can be attributed to the superiorities both in structure and in composition.

Introduction

Various core/shell structured nanospheres have been synthesized from various metal oxides, such as SnO_2 ,^{1,2} Fe_2O_3 ,^{3,4} and NiO .^{5,6} Their unique morphology containing a hollow space enables their application in various fields such as sensors,⁷ catalysts,³ and energy storage devices.^{1,8,9} Two different methodologies have been intensively studied to create inner spaces in such structures, including template-assisting method and template-free method. Some typical template-free methods, such as Ostwald ripening,¹⁰ Kirkendall type diffusion,¹¹ and chemically induced self-transformation¹² are competitive in terms of convenience and economy, because these methods do not need to sacrifice templates. However, with template-free methods it can be difficult to fabricate structures with perfect uniformity and controllability. On the other hand, traditional template-assisting methods usually involve multiple sacrificial templates, such as block copolymers, amphiphilic micellar scaffolds and colloidal silica. Therefore, a template removal process is always required, which may also lead to the exposure of the core part and the incompleteness of the shell part.^{13–18} A strategy to effectively solve the dilemma is to use a non-sacrificial template method to yield a satisfactory structure, in which the template is not sacrificed

but used for the formation of the product. Here, we report such a method for the synthesis of core/shell nanospheres.

As a typical transition metal oxide, Cr_2O_3 -based nanospheres with a core/shell structure have presented significant results in application to photocatalysis and magnetics.^{19–21} Recently, Cr_2O_3 has been suggested as a promising candidate for negative electrode materials of the Li-ion battery due to its high theoretical specific lithium storage capacity (1058 mA h g⁻¹) and relatively low lithium insertion potential among metal oxides (MO_x).^{22,23} Chromium is also adopted in cathode materials to increase the reversible capacity at a suitable content.²⁴ However, the application of Cr_2O_3 is clogged with a sharp capacity fade which is considered to be caused by the huge volume variation, pulverization, electronic contact lost and formation of unstable solid electrolyte interphase (SEI) during the Li uptake/release process. Several strategies have been proposed to solve these problems including decreasing the particles size, mesoporous structure design, carbon coating and using thin films.^{25–28} Among all these strategies, carbon coating is expected to be the most promising to enhance the electronic conductivity of the material and increase the stability of the SEI films.

A traditional carbon coating method is composed of two steps, the preparation of metal oxides and the hydrolysis process at high temperature.²⁹ For the structure design of electrode materials for Li-ion batteries, core/shell and mesoporous structures are always efficient for supplying cavities and paths for the electrolyte to diffuse quickly.^{26,30–32} However, few researchers have succeeded in the synthesis of hierarchical core/shell structured Cr_2O_3 -carbon composites (Cr_2O_3 -C) for lithium storage.

Here, Cr_2O_3 -based nanomaterials with different morphologies and compositions have been synthesized with a facile, soft, but non-sacrificial template of polyethylene glycol (PEG) with the assistance of $\text{H}_2\text{C}_2\text{O}_4$. Mesoporous Cr_2O_3 nanospheres and Cr_2O_3 -C hierarchical core/shell nanospheres can be easily obtained by taking controllable annealing parameters such as the

^aCAS Key Laboratory of Molecular Nanostructure and Nanotechnology, Institute of Chemistry, Chinese Academy of Sciences (CAS), Beijing, 100190, China. E-mail: ygguo@iccas.ac.cn; Fax: +(86)10-62557908; Tel: +(86)10-62557908

^bBeijing National Laboratory for Molecular Sciences (BNLMS), Beijing, 100190, China

^cBeijing National Laboratory for Condensed Matter Physics, Institute of Physics, Chinese Academy of Sciences, Beijing, 100190, China

† Electronic supplementary information (ESI) available: SEM images of the Cr_2O_3 precursor. TG curve of the sample. SEM and high-magnification SEM images of the Cr_2O_3 -comm. Elemental maps of Cr_2O_3 -C. Nitrogen adsorption/desorption isotherms of mesoporous Cr_2O_3 . See DOI: 10.1039/c0jm01027h/

atmosphere and temperature. Among three Cr_2O_3 -based samples, the Cr_2O_3 -C hierarchical core/shell nanospheres containing carbon nanocoating layers exhibit the best electrochemical performance for reversible lithium storage because of the unique morphology and the existence of carbon coating layers not only on the surface of particles but also encapsulated in the space formed by adjacent Cr_2O_3 nanoparticles.

Experimental section

Preparation of Cr_2O_3 -based composites

In a typical synthesis, 0.35 g of $\text{H}_2\text{C}_2\text{O}_4$ was dispersed into a mixed solution containing 7 mL of ethanol and 21 mL of polyethylene glycol (PEG, Mw = 380 ~ 420) under stirring. 0.8 g of $\text{Cr}(\text{NO}_3)_3 \cdot 9\text{H}_2\text{O}$ was introduced into the solution when the $\text{H}_2\text{C}_2\text{O}_4$ was dissolved completely, followed by adding 0.45 g of urea. The mixture of the above suspension and solution was transferred and sealed into a 40 mL Teflon-lined autoclave, then heated at 180 °C for 5 h after all the additives were dissolved completely. The precipitate was collected and washed with ethanol. The products were heated in a quartz tube at 750 °C for 6 h under H_2 (5 wt% in Argon) for preparing the Cr_2O_3 -C and 500 °C for 2 h under air to obtain the mesoporous Cr_2O_3 sample.

Characterization

X-ray diffraction (XRD) analysis was performed with a Rigaku D/max-2500 using filtered Cu-K α radiation. A Tecnai G2 F20 UTWI transmission electron microscope (TEM and HRTEM, operating at 200 kV) and a JEOL model 6701F field-emission scanning electron microscope (SEM, operating at 10 kV) were used to investigate the morphology and size of the as-obtained products. Thermogravimetric (TG) analysis was carried out using Perkin-Elmer model Pyris 1 thermal analysis equipment. Raman measurements were performed using a Digilab FTS3500 from Bio-Rad with a laser wavelength of 514.5 nm.

Electrochemical characterization

Electrochemical measurements were performed using two-electrode Swagelok type cells assembled in an argon-filled glove box. For preparing working electrodes, a mixture of active material, acetylene black, and poly(vinyl difluoride) (PVDF) at a weight ratio of 80 : 10 : 10 was pasted on a copper foil. A glass fiber (GF/D) from Whatman was used as a separator. Lithium foil was used as the counter electrode. The electrolyte consisted of a solution of 1M LiPF₆ in ethylene carbonate (EC)/dimethyl carbonate (DMC)/diethyl carbonate (DEC) (1 : 1 : 1 in wt%) was obtained from Tianjin Jinniu Power Sources Materials Co., Ltd. Galvanostatic cycling tests of the assembled cells were carried out on a LAND system in the voltage range of 0.02–3.0 V (vs Li⁺/Li) at a discharge/charge rate of C/5.

Results and discussion

Fig. 1a shows the XRD patterns of as-prepared Cr_2O_3 samples treated in air and H_2 respectively, and the XRD pattern of commercial Cr_2O_3 bought from Beijing Chemicals Co. Ltd (referred to as Cr_2O_3 -com) is also presented for comparison. In

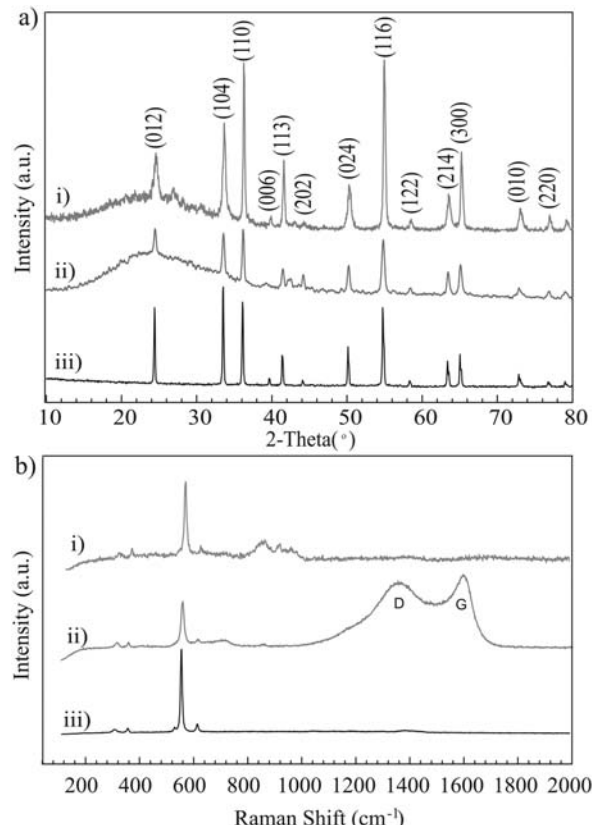


Fig. 1 (a) XRD patterns of (i) mesoporous Cr_2O_3 , (ii) Cr_2O_3 -C, (iii) Cr_2O_3 -com; (b) Raman spectra of (i) mesoporous Cr_2O_3 , (ii) Cr_2O_3 -C, (iii) Cr_2O_3 -com.

the following, mesoporous Cr_2O_3 , Cr_2O_3 -C, and Cr_2O_3 -com refer to the three types of Cr_2O_3 -based samples. The XRD patterns indicate that all the diffraction peaks are in good agreement with the eskolaite structure (JCPDS No. 38-1479) with the cell parameters: $a = 4.958 \text{ \AA}$, $c = 13.594 \text{ \AA}$, S.G. = $R-3c$. No impurity phase is found either in the mesoporous Cr_2O_3 or the Cr_2O_3 -C sample.

As shown in the Raman spectra in Fig. 1b, the G band and D band of carbon can be only observed in the Cr_2O_3 -C sample. This indicates that the carbon precursor in the mesoporous Cr_2O_3 sample has been burned completely, but has pyrolyzed in the Cr_2O_3 -C sample, in contrast. The remaining carbon shows poor crystallinity according to the low ratio of relative intensities of the G-band to D-band and the absence of graphite peak in the XRD pattern of Cr_2O_3 -C sample.

SEM and TEM images have further revealed the morphology of as-prepared Cr_2O_3 -based materials. The precursors of Cr_2O_3 before heat treatment are microspheres with a smooth surface and uniform diameter of about 1 μm (Fig. 2a). The surface becomes relatively rough and many pores appear after annealing under air atmosphere, as clearly shown in Fig. 2b and 2c. N_2 adsorption-desorption isotherms of the sample exhibit typical IV isotherms with a hysteresis loop, which are typical characteristics of mesoporous materials (see Fig. S5†), confirming the existence of mesopores. The Barrett-Joyner-Halenda (BJH) pore size distribution (inset in Fig. S5†) indicates that the mesoporous

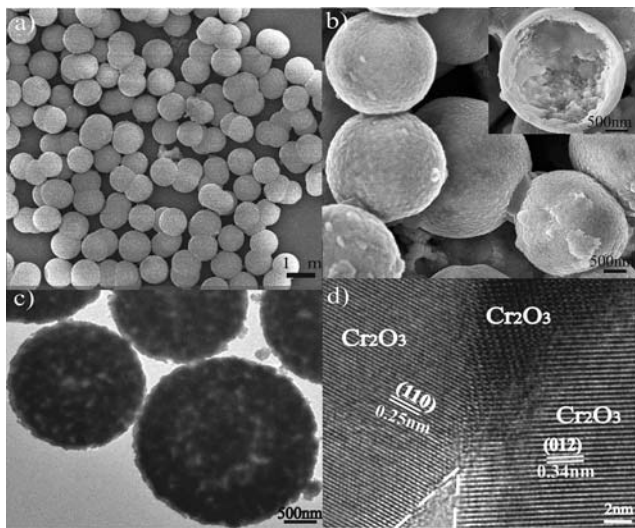


Fig. 2 SEM images of (a) Cr_2O_3 precursor, (b) mesoporous Cr_2O_3 . (c) TEM, and (d) HRTEM images of mesoporous Cr_2O_3 . The inset in (b) shows the SEM image of a broken sphere indicating its inside structure.

Cr_2O_3 exhibit two types of pores with different average diameters of 7.7 and 30.7 nm. A representative high-resolution TEM (HRTEM) image is shown in Fig. 2d. The lattice fringes are clearly visible with a spacing of 0.25 nm and 0.34 nm, respectively, corresponding to the spacing of the (110) and (012) planes of eskolaite Cr_2O_3 . The appearance of pores inside the mesoporous Cr_2O_3 is resulted from the combustion of the carbon-containing precursor.

Different from the mesoporous structures of spheres in the mesoporous Cr_2O_3 sample, the morphology changes into hollow core/shell structures after annealing under H_2 , as shown in Fig. 3a and 3b. The pyrolyzed carbon can be seen both on the surface of the particles and inside the particles (Fig. 3b–d). The terminal core/shell structure is assembled by the Cr_2O_3

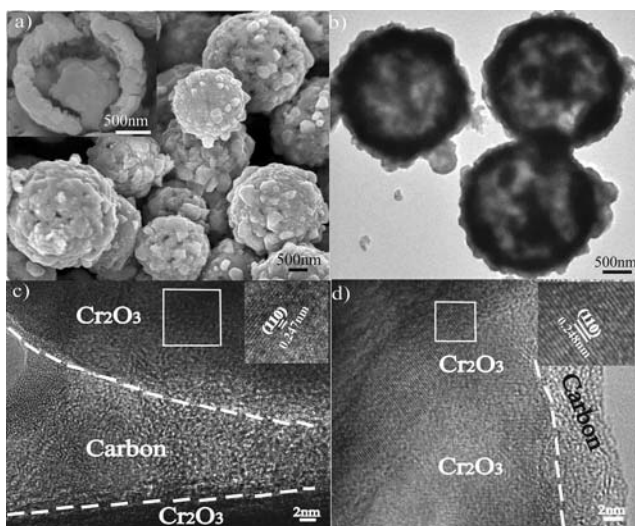


Fig. 3 SEM images of (a) $\text{Cr}_2\text{O}_3-\text{C}$, (b) TEM images of $\text{Cr}_2\text{O}_3-\text{C}$; and (c, d) HRTEM images of $\text{Cr}_2\text{O}_3-\text{C}$. The inset in (a) shows the SEM image of a broken sphere indicating its core-shell structure.

nanostructures coated by carbon layers to form a hierarchical core/shell structure. The carbon nanocoating layers form interconnected and continuous networks with uniform distribution from the inside to the surface, which is a unique feature of the product obtained via the facile method, as confirmed by EDX maps covering a large number of particles (see Fig. S4†). This is essential to maintain the internal electronic contact of particles during the charging and discharging process, especially for insulating electrode materials with high capacity. For example, high capacity Sn–Co–C anode materials invented by SONY company where Sn–Co alloy nanograins are dispersed in amorphous carbon matrix show excellent cycle performance.³³ Among transition metal oxide anode materials, this approach is realized for the first time and is different from the simple carbon coating strategy previously reported wherein the carbon layers merely cover the particle surface.^{25,31,34}

In order to clarify the function of PEG and $\text{H}_2\text{C}_2\text{O}_4$, the synthesis experiments were also performed in the absences of PEG or $\text{H}_2\text{C}_2\text{O}_4$. As can be seen from Fig. S1†, the products exhibited morphologies of small nanoparticles and large composites rather than uniform nanospheres in these cases. It is obvious that PEG and $\text{H}_2\text{C}_2\text{O}_4$ are two key morphology-controlling factors, while the reaction medium of water or ethanol is not essential because microspheres can still be obtained when water or ethanol is absent. Similar to the typical EG-mediated process where the ethylene glycol units are the media leading to the formation of longer chains through several steps of intermediated reaction, the ethylene glycol units in the long chains of PEG could also coordinate with $\text{Cr}(\text{NO}_3)_3$ in the existence of $\text{H}_2\text{C}_2\text{O}_4$ to form the chromium glycolates in our experiment.³⁵ It was found that the yield of the solid precursor was much lower when urea was absent. The result indicates that the urea might provide an alkali solution and hence promotes the formation of the chromium glycolates. Another function of PEG and $\text{H}_2\text{C}_2\text{O}_4$ is that they can be used as the carbon precursor for the final products. TG analysis shows that the carbon content is 3 wt% in the $\text{Cr}_2\text{O}_3-\text{C}$ sample (see Fig. S2†).

Fig. 4a presents the first discharge/charge voltage profiles for the Cr_2O_3 -based materials. Among the three samples, the $\text{Cr}_2\text{O}_3-\text{C}$ obviously has the highest reversible capacity (charge capacity) of 688 mA h g^{-1} at a rate of C/5 between the voltage limits of 0.02–3.0 V (vs Li⁺/Li). The outstanding performance could be attributed to two factors. Firstly, the unique core/shell structure provides certain space which is helpful for the electrolyte to diffuse quickly. Secondly, the carbon layers encapsulated inside the particles is favorable to maintain internal electronic contact of particles so as to increase the utilization of active materials of Cr_2O_3 .

Furthermore, the $\text{Cr}_2\text{O}_3-\text{C}$ also possesses the best cycle performance as revealed by Fig. 4b. Even after 35 cycles, the reversible capacity for $\text{Cr}_2\text{O}_3-\text{C}$ still retains more than 600 mA h g^{-1} , showing a capacity retention of 87%, while mesoporous Cr_2O_3 and Cr_2O_3 -com can only deliver a capacity of 320 mA h g^{-1} and 280 mA h g^{-1} , respectively. The capacity retention of $\text{Cr}_2\text{O}_3-\text{C}$ is much better than the reported mesoporous Cr_2O_3 ²⁶ and Cr_2O_3 -carbon composite.²⁵ In brief, such special $\text{Cr}_2\text{O}_3-\text{C}$ composite nanospheres with core/shell structure surpass mesoporous Cr_2O_3 without carbon coating layers and show superiority to $\text{Cr}_2\text{O}_3-\text{C}$ without a particular designed structure.

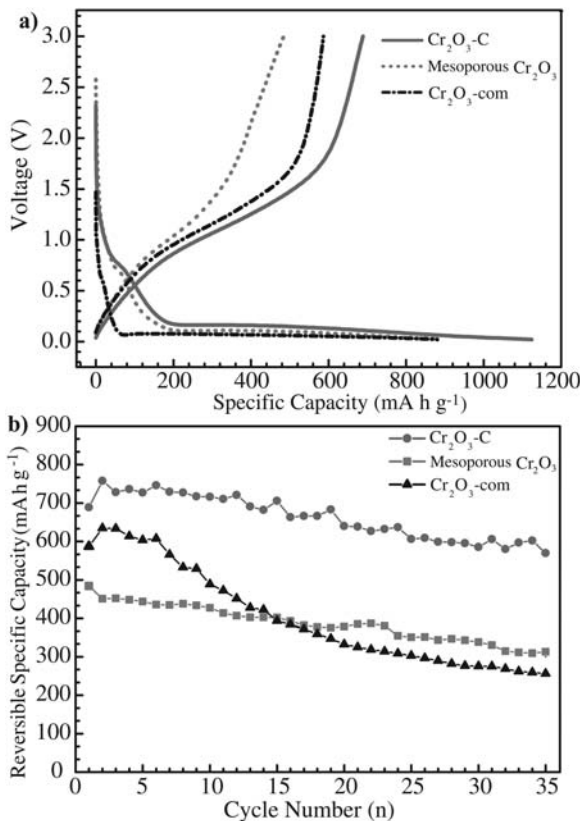


Fig. 4 a) The first discharge/charge voltage profiles, and b) cycle performance of Cr₂O₃-C, mesoporous Cr₂O₃, and Cr₂O₃-com.

In detail, the main reasons for the enhanced cycle performance could be concluded as follows: (i) The carbon layers, as well as the existence of a cavity within the spheres may help to alleviate the volume change during the charge/discharge process. (ii) The carbon layers inside may help to maintain the integral structure of nanospheres thus preventing them from pulverization, while also keeping the interparticle electronic contact for each sphere. This is especially essential for insulating active material like Cr₂O₃ in which large volume variation and significant phase transition may occur during lithium insertion and extraction process. (iii) The SEI films formed on the Cr₂O₃-C surface are relatively stable. It should be noted that the performance might be further improved if the carbon coating process is followed by a CVD method to cover the particle surface uniformly, and this will be investigated in the near future.

Conclusions

In summary, we report a facile soft-template assisted method to synthesize Cr₂O₃-based nanospheres without sacrificing the template. By using a certain thermal treatment, Cr₂O₃-C composite nanospheres with a novel hierarchical core/shell structure and pure mesoporous Cr₂O₃ spheres can be obtained. PEG and H₂C₂O₄ are two key components in the self-assembly process of the sphere-like morphology, as well as the production of carbon in the final composite materials. Especially, nanospheres in the Cr₂O₃-C sample exhibit unique core/shell structures with carbon coating layers continuously distributed from the inside to the surface of the spheres. The superiorities both in

structure and in composition may improve the lithium storage capacity dramatically. The nano-sized cavity existed in the core/shell structure may accommodate the volume variation and may be beneficial to the diffusion of liquid electrolyte. The carbon layers may also alleviate the volume change while leading to the formation of relatively stable SEI during Li⁺ insertion/extraction. Most importantly, the inside carbon layers maintain internal electronic contact among active nanoparticles of Cr₂O₃ during the charging and discharging cycles. Both the synthesis and the structure design strategies might also be extended to other anode and cathode materials for lithium-ion batteries.

Acknowledgements

This work is supported by the National Natural Science Foundation of China (Grant No. 50730005, 20821003 and 20701038), National Key Project on Basic Research (Grant No. 2009CB930400), and the Knowledge Innovation Program of the Chinese Academy of Sciences (No. KJCX2-YW-W26).

Notes and references

- M. Li, Q. H. Lu, Y. Nuli and X. F. Qian, *Electrochim. Solid-State Lett.*, 2007, **10**, K33–K37.
- D. Deng and J. Y. Lee, *Chem. Mater.*, 2008, **20**, 1841–1846.
- L. M. Lang, B. J. Li, W. Liu, X. Li and Z. Xu, *Chem. Lett.*, 2009, **38**, 806–807.
- L. Xiang, Y. P. Yin and Y. Jin, *J. Solid State Chem.*, 2004, **177**, 1535–1541.
- I. S. Lee, N. Lee, J. Park, B. H. Kim, Y. W. Yi, T. Kim, T. K. Kim, I. H. Lee, S. R. Paik and T. Hyeon, *J. Am. Chem. Soc.*, 2006, **128**, 10658–10659.
- A. C. Johnston-Peck, J. W. Wang and J. B. Tracy, *ACS Nano*, 2009, **3**, 1077–1084.
- J. Zhang, S. R. Wang, M. J. Xu, Y. Wang, H. J. Xia, S. M. Zhang, X. Z. Guo and S. H. Wu, *J. Phys. Chem. C*, 2009, **113**, 1662–1665.
- W. J. Cui, F. Li, H. J. Liu, C. X. Wang and Y. Y. Xia, *J. Mater. Chem.*, 2009, **19**, 7202–7207.
- H. Kim and J. Cho, *Nano Lett.*, 2008, **8**, 3688–3691.
- H. C. Zeng, *J. Mater. Chem.*, 2006, **16**, 649–662.
- Y. D. Yin, R. M. Rioux, C. K. Erdonmez, S. Hughes, G. A. Somorjai and A. P. Alivisatos, *Science*, 2004, **304**, 711–714.
- J. G. Yu, H. T. Guo, S. A. Davis and S. Mann, *Adv. Funct. Mater.*, 2006, **16**, 2035–2041.
- M. E. Davis, *Nature*, 2002, **417**, 813–821.
- B. Jin Ho and S. S. Kenneth, *Adv. Mater.*, 2009, **21**, 3186–3190.
- A. Wolosiuk, O. Armagan and P. V. Braun, *J. Am. Chem. Soc.*, 2005, **127**, 16356–16357.
- M. F. Zhang, M. Drechsler and A. H. E. Muller, *Chem. Mater.*, 2004, **16**, 537–543.
- I. Yamaguchi, M. Watanabe, T. Shinagawa, M. Chigane, M. Inaba, A. Tasaka and M. Izaki, *ACS Appl. Mater. Interfaces*, 2009, **1**, 1070–1075.
- A. K. Sinha and K. Suzuki, *Angew. Chem., Int. Ed.*, 2005, **44**, 271–273.
- K. Maeda, K. Teramura, D. L. Lu, N. Saito, Y. Inoue and K. Domen, *Angew. Chem., Int. Ed.*, 2006, **45**, 7806–7809.
- K. Maeda, K. Teramura, D. L. Lu, N. Saito, Y. Inoue and K. Domen, *J. Phys. Chem. C*, 2007, **111**, 7554–7560.
- G. Xiong, A. G. Joly, G. P. Holtom, C. M. Wang, D. E. McCready, K. M. Beck and W. P. Hess, *J. Phys. Chem. B*, 2006, **110**, 16937–16940.
- J. Hu, H. Li and X. J. Huang, *Electrochim. Solid-State Lett.*, 2005, **8**, A66–A69.
- S. Grangeon, S. Laruelle, L. Dupont, F. Chevallier, P. L. Taberna, P. Simon, L. Gireaud, S. Lascaud, E. Vidal, B. Yrieix and J. M. Tarascon, *Chem. Mater.*, 2005, **17**, 5041–5047.
- I. R. Mangani, C. W. Park, S. H. Kim and J. Kim, *J. Power Sources*, 2006, **158**, 1405–1409.

- 25 J. Hu, H. Li, X. J. Huang and L. Q. Chen, *Solid State Ionics*, 2006, **177**, 2791–2799.
- 26 L. Dupont, S. Gruegeon, S. Laruelle and J. M. Tarascon, *J. Power Sources*, 2007, **164**, 839–848.
- 27 L. Dupont, S. Laruelle, S. Gruegeon, C. Dickinson, W. Zhou and J. M. Tarascon, *J. Power Sources*, 2008, **175**, 502–509.
- 28 J. P. Sun, K. Tang, X. Q. Yu, J. Hu, H. Li and X. J. Huang, *Solid State Ionics*, 2008, **179**, 2390–2395.
- 29 W. M. Zhang, X. L. Wu, J. S. Hu, Y. G. Guo and L. J. Wan, *Adv. Funct. Mater.*, 2008, **18**, 3941–3946.
- 30 H. S. Zhou, D. L. Li, M. Hibino and I. Honma, *Angew. Chem., Int. Ed.*, 2005, **44**, 797–802.
- 31 W. M. Zhang, J. S. Hu, Y. G. Guo, S. F. Zheng, L. S. Zhong, W. G. Song and L. J. Wan, *Adv. Mater.*, 2008, **20**, 1160–1166.
- 32 D. L. Li, H. S. Zhou and I. Honma, *Nat. Mater.*, 2004, **3**, 65–72.
- 33 S. Kawakami and M. Asao, EP1039568-A, 2000.
- 34 L. Y. Jiang, X. L. Wu, Y. G. Guo and L. J. Wan, *J. Phys. Chem. C*, 2009, **113**, 14213–14219.
- 35 Y. L. Wang, X. C. Jiang and Y. N. Xia, *J. Am. Chem. Soc.*, 2003, **125**, 16176–16177.

Supplementary Material (ESI) for Journal of Materials Chemistry

This journal is (c) The Royal Society of Chemistry 2010

Electronic Supplementary Information for

Non-sacrificial template synthesis of Cr₂O₃-C hierarchical core/shell nanospheres and their application as anode materials in lithium-ion batteries

Ling-Yan Jiang,^a Sen Xin,^a Xing-Long Wu,^a Hong Li,^b Yu-Guo Guo^{a*} and Li-Jun Wan^a

^a *CAS Key Laboratory of Molecular Nanostructure and Nanotechnology, Institute of Chemistry, Chinese Academy of Sciences (CAS), Beijing 100190, China.*

Beijing National Laboratory for Molecular Sciences (BNLMS), Beijing 100190, China

^b *Beijing National Laboratory for Condensed Matter Physics, Institute of Physics, Chinese Academy of Sciences, Beijing 100190, China.*

* Corresponding author. E-mail: yguo@iccas.ac.cn, Tel. & Fax: (86)10-62557908

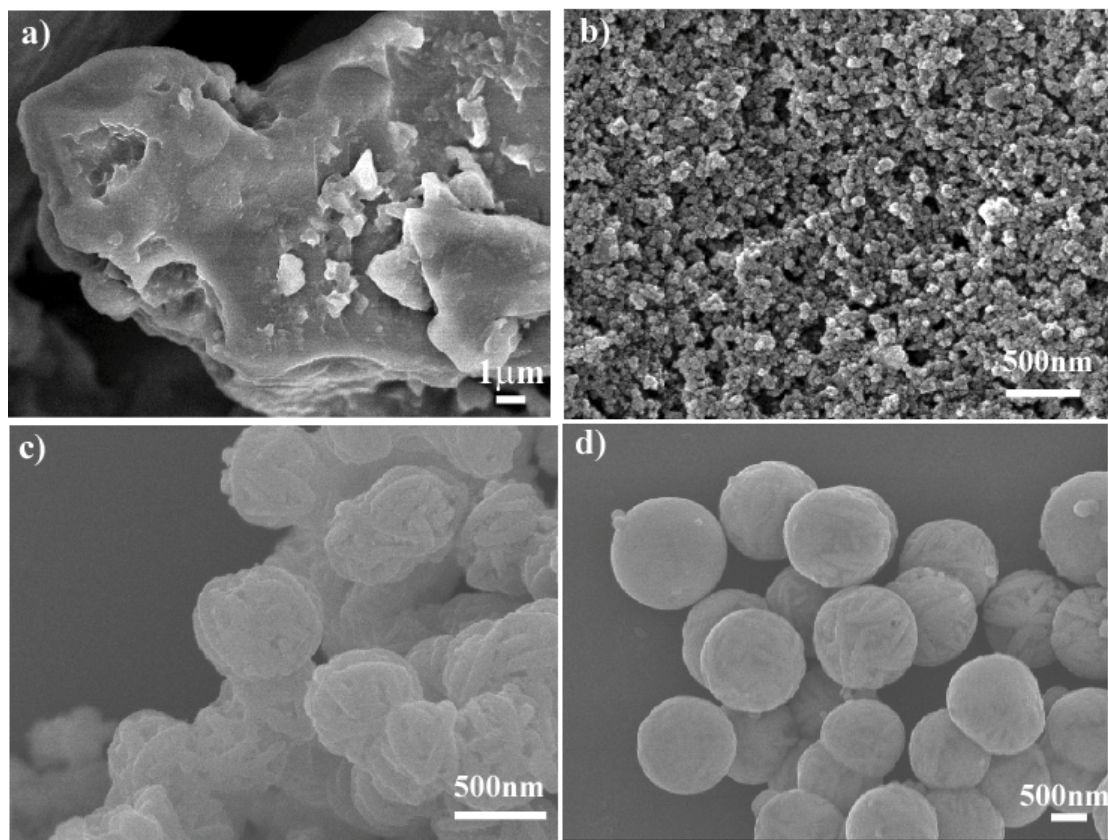


Figure S1. SEM images of a) as-prepared product without PEG, b) as-prepared product without $\text{H}_2\text{C}_2\text{O}_4$, c) as-prepared product without H_2O , and d) as-prepared product without ethanol annealed under N_2 .

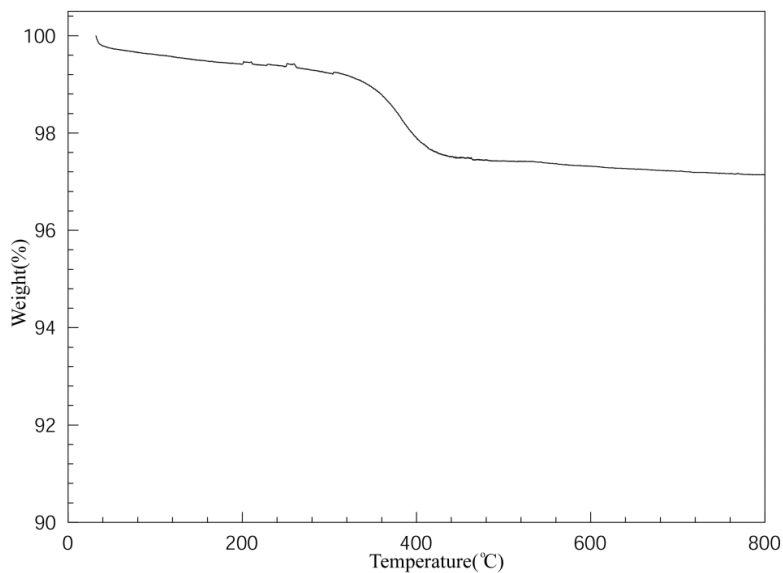


Figure S2. TG curve of the $\text{Cr}_2\text{O}_3\text{-C}$ sample. (Tested in air with the temperature raising speed of 10 °C

min^{-1}).

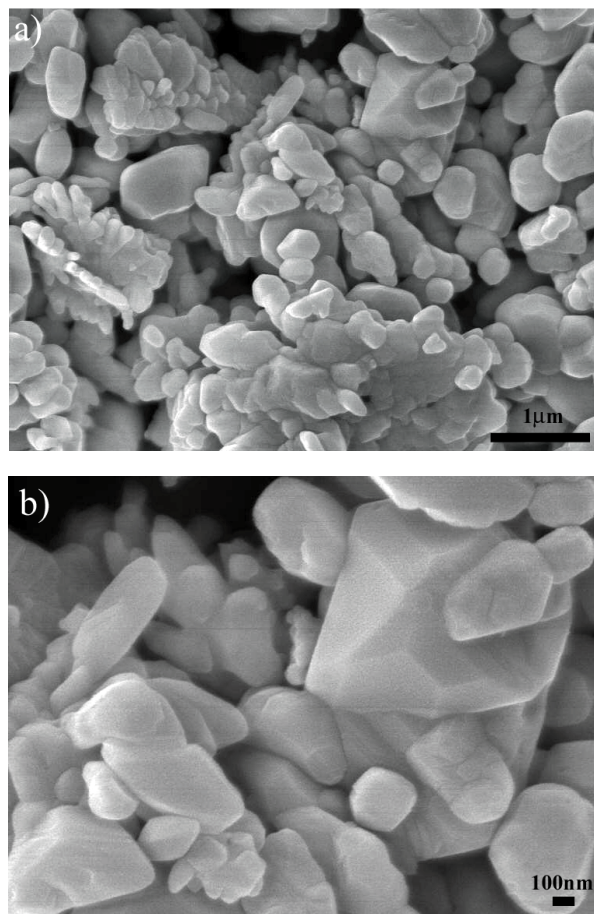


Figure S3. a) SEM and b) high-magnification SEM images of the Cr₂O₃-com.

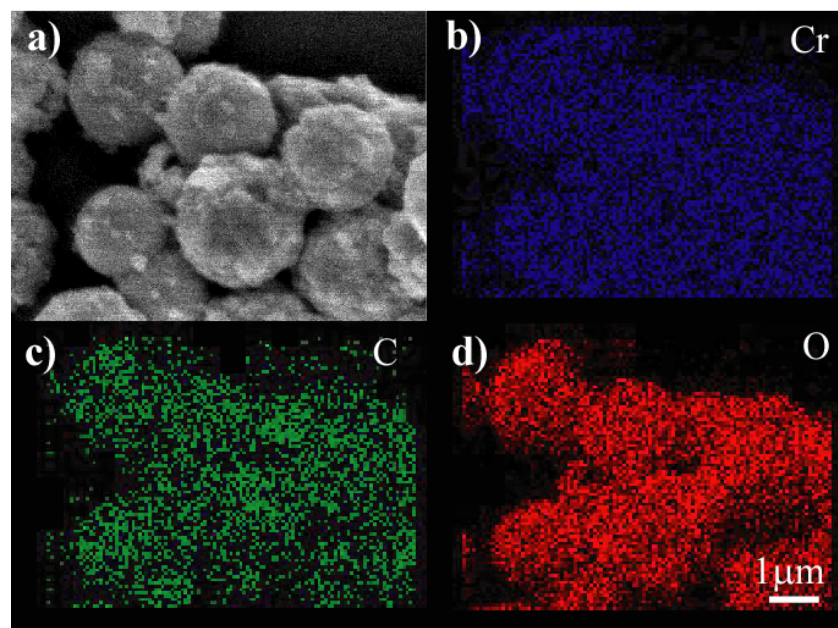


Figure S4. a) SEM image of the Cr_2O_3 -C composite and corresponding b) Cr, c) C and d) O EDX maps.

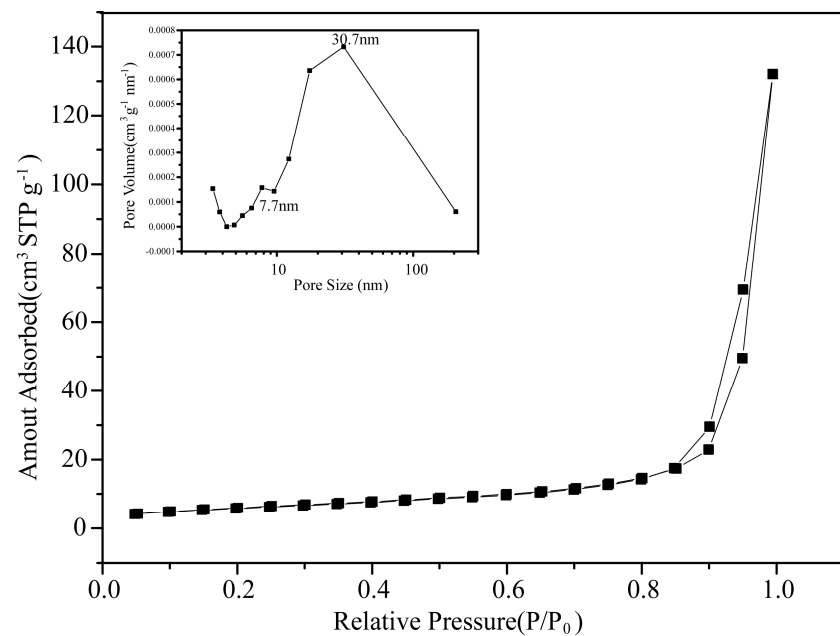


Figure S5. Nitrogen adsorption/desorption isotherms of mesoporous Cr_2O_3 . Inset shows the pore size distribution plot which was calculated according to the BJH formula.